American Mineralogist, Volume 110, pages X-XX, 2025

Structural variations along the apatite F-OH join: II. The role of hydrogen bonding in fluoridated teeth

John M. Hughes[1,2,*], Daniel Harlov[3,4,5,†], John F. Rakovan[2,6], Jamshid Ahmadi[2], and Melanie J. Sieber[3,7]

[1]Department of Geology, University of Vermont, Burlington, Vermont 05405, U.S.A.
[2]Department of Geology & Environmental Earth Sciences, Miami University, Oxford, Ohio 45056, U.S.A.
[3]Deutches GeoForschungsZentrum GFZ, Telegrafenberg, D-14473 Potsdam, Germany
[4]Faculty of Earth Resources, China University of Geosciences, 430074 Wuhan, China
[5]Department of Geology, University of Johannesburg, P.O. Box 524, Auckland Park, 2006, South Africa
[6]New Mexico Bureau of Geology and Mineral Resources, New Mexico Tech, 801 Leroy Place, Socorro, New Mexico 87801, U.S.A.
[7]University of Potsdam, Institute of Geosciences, Karl-Liebknecht-Strasse 24-25, D-14476 Potsdam, Germany

Abstract

Fluoride is one of the most consumed pharmaceuticals in the world, and its facility in preventing dental caries is recognized as one of the top 10 public health achievements of the 20th century. Although hydroxylapatite is often used as an analog of dental enamel, the details of the substitution of F for OH in the apatite anion column are not well known. Using new synthesis techniques, this study extends the structure work on $P6_3/m$ apatites along the middle portion of the F-OH apatite join to compositions near the composition of fluoridated human teeth. The first F substituent in hydroxylapatite, near fluoridated dental enamel compositions, is dramatically underbonded by the surrounding Ca2 atoms (0.72 v.u.) in a hydroxylapatite matrix. However, the hydroxyl hydrogen can contribute 0.20 or 0.10 v.u. in hydrogen bonding, depending on whether the substitution creates a reversal site in the anion column; this hydrogen bonding alleviates the bonding requirements of the substituent F. As F concentrations increase along the join, the average hydroxyl contributes increasing amounts of hydrogen bonding to the F column anions; to mitigate the loss of its hydrogen bonding, the hydroxyl oxygen migrates toward the adjacent mirror plane that contains the bonded Ca2 atoms, and the triangle of bonded Ca2 ions concomitantly contracts. These two mechanisms increase bonding to the column hydroxyl oxygen from the adjoining Ca2 atoms to balance the loss of hydrogen bonding that stabilizes the substituent F column anion and the increasing concentration of underbonded F.

Keywords: Hydroxylapatite, fluoridation, crystal structure, teeth

Introduction

A pharmaceutical can be defined as a compound that is used to prevent, treat, or cure a disease; among the most widely administered pharmaceuticals is fluoride (the ionic form of fluorine), administered in several forms. Indeed, in 2018, 73.0% of the U.S. population consumed water from community water systems that contain fluoridated water (CDC 2021) to prevent dental caries. Community water fluoridation is recognized as one of the 10 greatest public health achievements of the 20th century, preventing at least 25% of tooth decay in adults and children (American Public Health Association 2021).

Understanding how a pharmaceutical compound interacts with the human body is fundamental to administering pharmaceuticals. Although there are models that conjecture on how the addition of fluoride to the outermost unit cells of human dental enamel can prevent dental caries, there are no quantitative measurements of the changes in the atomic arrangement or bonding that occur in response to fluoridation; human teeth are not well crystallized or suitable for the high-precision diffraction studies that are necessary to understand the atomic-level interactions with fluorine as a pharmaceutical.

It is well known that inorganic hydroxylapatite, natural or synthetic $Ca_{10}(PO_4)_6(OH)_2$, is an analog for human dental enamel, although the latter also contains several percent of the carbonate anionic complex (Leventouri et al. 2009). Natural mineral samples of hydroxylapatite are not particularly useful in examining detailed atomic arrangements as they apply to human teeth. Mineral samples are inherently mixtures of the three anionic end-members of apatite, $Ca_{10}(PO_4)_6(OH,F,Cl)_2$, and pure OH end-member minerals are unknown. Even the putative natural hydroxylapatite end-member from Holly Springs, Georgia, U.S.A., has been shown to contain both F and Cl in the anion column, obviating direct comparisons to human dental apatite (Dykes and Elliott 1971). For this reason, Hughes et al. (2018) attempted to synthesize apatite samples along the F-OH join and reported the detailed atomic arrangements of apatites in the mid-solid solution range, with anion compositions between and including $[F_{40}(OH)_{60}]$ and $[F_{67}(OH)_{33}]$. However, the attempts to synthesize less F-rich hydroxylapatite to mimic and elucidate the atomic changes that occur with the addition of F to hydroxylapatite through fluoridation were not successful, thus they reported on the middle range of the fluorapatite-hydroxylapatite

* Corresponding author E-mail: jmhughes@uvm.edu
† Orcid https://orcid.org/0009-0009-0836-219X

0003-004X/25/0003–xxx$05.00/DOI: https://doi.org/10.2138/am-2024-9393

solid solution only; synthesis of hydroxylapatite with small amounts of substituent F is difficult, particularly with a yield of crystals suitable for single-crystal diffraction studies.

Since that publication, new methods of synthesizing hydroxylapatite with lower F concentrations of sufficient size for single-crystal study have been devised, and details of that synthesis are given below. The addition of the atomic arrangement of samples with compositions as low as ~$[F_{10}(OH)_{90}]$ allows us to conjecture on the incorporation of small amounts of F in hydroxylapatite and comment on the bonding that occurs with the fluoridation of human teeth.

Fluoridation of Hydroxylapatite in Teeth

The mechanism(s) by which F^- reduces the incidence of dental caries have been investigated in thousands of studies over the last half-century. Numerous reviews on this topic have been published (e.g., Featherstone 1999; Aoun et al. 2018; Epple et al. 2022; ten Cate and Buzalaf 2019). Although numerous mechanisms have been suggested, a high degree of consensus exists on the following: (1) promotion of remineralization (new apatite formation after partial dissolution of original tooth material); (2) formation of fluoridated hydroxylapatite during remineralization, and with less CO_3 than the original tooth apatite; (3) antimicrobial properties, affecting bacteria growth and metabolism; (4) surface armoring by F^- sorption to dental hydroxylapatite inhibiting dissolution; (5) F^- incorporation in pre-eruptive tooth apatite, depending on the amount of F^- ingestion, though it is thought to be negligible in preventing dental caries.

Although there are still many questions to be answered, there is sufficient evidence that fluoridated hydroxylapatite, with variable amounts of other substituents (e.g., CO_3), can be created in teeth by engineered exposure to F^- (reviews cited above). This may be through the process of diffusion of sorbed F^- into tooth apatite (only in the surface-most regions of crystallites). It is thought that a more important mechanism of fluoridated hydroxylapatite formation is the dissolution (demineralization) of original tooth apatite and reprecipitation (remineralization) of new F^--doped hydroxylapatite. Fluoridated hydroxylapatite has a lower solubility than the non-fluoridated species. It is believed that one mechanism for F^- reduction of dental caries is by decreasing the susceptibility of fluoridated hydroxylapatite in teeth to acid dissolution as a result of its lower solubility compared to non-fluoridated tooth apatite.

Experimental Methods

Synthesis of the four low-F samples

The eight most F-rich samples shown in the accompanying figures {between $[F_{40}(OH)_{60}]$ and $[F_{67}(OH)_{33}]$} were reported in Hughes et al. (2018), and that paper contains the experimental details for the synthesis of those samples as well as the sample with composition $[F_{17}(OH_{83})]$, i.e., the most F-rich of the four low-F samples.

We encountered difficulty in synthesizing low-F crystals using the methods detailed in the previous work, and several years were spent attempting such samples. Using the synthesis methods outlined below, we successfully synthesized samples with compositions as low as ~$(F_{0.10}OH_{0.90})$, significantly extending the range of samples from the middle portion of the binary join reported earlier. These new syntheses included samples APS-110, APS-125, APS-126, and APS-127a with F contents lower than the hydroxyl-fluorapatites reported by Hughes et al. (2018).

Synthesis of these four fluoridated hydroxylapatite compositions was undertaken at GeoForschungsZentrum, Potsdam, Germany; the syntheses were accomplished by mixing commercial-grade hydroxylapatite (1 μm particle size) with NaF in gram amounts to ensure a low weighing error. This nominally consisted of 9.5–10 g of hydroxylapatite +0.01–0.02 g of NaF mixed with ethanol in an agate mortar using an agate pestle continuously by hand for about 15 min to ensure a homogeneous mixture. The hydroxylapatite-NaF mix was then dried at 105 °C for about an hour. A random sampling of ~50–55 mg of this mix + 7 mg of H_2O was then added to a tempered (1000 °C), 3 mm diameter, 2 cm long Pt capsule that was arc-welded shut at one end. The H_2O was added first. The mix was then added and subsequently packed in. The Pt capsule was then arc-welded shut, placed in the 105 °C oven for 5–10 h, and weighed again to check for leaks. Any capsule showing weight loss >0.02 mg was discarded.

The four synthesis experiments were run at 1100 °C and 300 MPa in the internally heated gas pressure vessel (IHGPV) for 8 days. An example (APS-126) of the basic reaction between the hydroxylapatite and the NaF in an H_2O-rich environment (assuming total reaction) is as follows:

$$Ca_{10}(PO_4)_6(OH)_2 + 0.04\ NaF = Ca_{10}(PO_4)_6(OH_{0.98},F_{0.02})_2 + 0.04\ NaOH$$

All four synthesis capsules were run together at the same time. In the IHGPV, the temperature was measured with three S-type thermocouples and calibrated based on measurements of the melting points of NaCl at 843 °C/200 MPa and 904 °C/500 MPa (Akella et al. 1969). The accuracy is about ±5 °C at 200 MPa and ±20 °C at 500 MPa. Maximum thermal gradients along the capsules were ±10 °C. Pressure measurement was done with a strain gauge and was accurate to ±7 MPa for experiments up to 500 MPa. During the experiment, pressure was controlled automatically to within ±5 MPa using the hydraulic system of the intensifier and a programmable control unit. The samples were heated isobarically at a rate of 30 °C/min and quenched isobarically with quench rates of 150 to 200 °C/min. After the run, the very shiny and slightly deformed Pt capsules were removed, cleaned, and weighed. Any capsules showing weight loss (>0.05 mg) were discarded. The capsules were punctured, dried at 105 °C for several hours, and weighed again to determine fluid loss. The dry and recrystallized hydroxylapatite was removed from the Pt capsule, labeled, and stored.

X-ray structure studies

Data from the eight most F-rich samples presented here are taken directly from Hughes et al. (2018), and details of the X-ray structure studies, including Online Materials[1] CIF files, are contained or referenced therein. The structure of the sample of composition $[F_{17}(OH_{83})]$ was analyzed in the same laboratory using the same procedures detailed in the 2018 work, and the Online Materials[1] CIF for that sample is on deposit with the present study.

Crystals from the three samples with the lowest F contents were significantly smaller than the other samples, presumably due to the different synthesis conditions. To successfully undertake structure studies of those samples, a Bruker D8 Quest single-crystal X-ray diffractometer with a D8 three-circle goniometer, Mo microfocus (IμS) *K*α radiation, and a PHOTON III C7 area detector was employed. The CIF file (deposited in Online Materials[1]) contain crystal data and data collection/refinement parameters for the three lowest-F samples.

Bonding of the Apatite Column Anions: OH-F

In the $Ca_{10}(PO_4)_6(OH,F,Cl)_2$ system, the anion column accommodates three monovalent species, (OH), F, and Cl. Hughes et al. (1990) detailed the structural accommodation of all three species in hexagonal ternary apatite and demonstrated that a monoclinic ternary apatite also exists. Hughes et al. (2014) examined the details of the atomic arrangement along the F-Cl binary and the structural accommodation of the two anions of disparate size, and Hughes et al. (2016) elucidated the accommodation of Cl and OH along that binary apatite join and demonstrated that three different arrangements of the column anions exist. Hughes et al. (2018) examined the structure along the central portion of the F-OH apatite binary, a binary of particular interest in biological systems. As noted previously, the present work extends the results of Hughes et al. (2018) toward the

hydroxyl end-member and allows conclusions regarding the incorporation of substituent F in biological hydroxylapatite, such as occurs during the fluoridation of human teeth.

In compositions along the F-OH apatite join, two species occupy the anion column. Figure 1 illustrates the possible positions of the column occupants, OH and F, at two adjacent intersections of the (00*l*) mirror planes and [001] anion column. The mirror planes occur at z = ¼ and ¾ within each unit cell of $P6_3/m$ apatite, and at each intersection, one of three possible occupants can exist, each with bonds to the three Ca2 ions disposed in a triangle within the mirror plane. If an F ion occurs in that anion column, it lies coplanar in the mirror plane with the three Ca2 atoms. If a hydroxyl exists at that mirror plane, it will be displaced ~0.34 Å above or below the plane due to its slightly larger size (see depiction of OH_{above} and OH_{below} in Fig. 1), bonding to the three Ca2 atoms at slightly longer lengths than the aforementioned Ca-F bonds. In every case, the H atom of the hydroxyl is directed away from the mirror plane, leading to the possibility of hydrogen bonding within the anion column. Thus, of interest are the steric interactions between OH and F in neighboring sites in the anion column, particularly near the OH end of the F-OH join; that compositional region mimics the composition of fluoridated hydroxylapatite in teeth. Given the reported structures, we can examine the changes that occur with decreasing fluoridation along the fluorapatite-hydroxylapatite join, as well as calculate the strength and direction of the bonding impinging on each column anion. Keep in mind that the conclusions are based on X-ray structure studies that average over the entire crystal.

In pure hydroxylapatite, $[F_0(OH)_{100}]$, the hydroxyl in any individual anion column will be ordered as all OH_{above} or OH_{below}, as there are no vacancies or impurities to reverse the anion sequence at any of the column anion sites; this leads to $P2_1/b$ monoclinic apatite (Elliott et al. 1973). However, this has not been observed in geologic apatite, as sufficient impurities apparently exist to provide reversal sites for the hydroxyls, and there is probably sufficient Type A carbonate substitution in dental enamel to also provide reversal sites. However, the presence of monoclinic zones in hydroxylapatite does not obviate the discussion of hydrogen bonding in this work.

In pure hydroxylapatite, there is weak hydrogen bonding between adjacent hydroxyls that are ordered in the same sense, i.e., both OH_{above} or OH_{below}. For example, in Figure 1, a hydroxyl disordered below the plane at $z = ¾$ will lead to a neighboring OH_{below} associated with the adjacent mirror plane at $z = ¼$. The O─O distance will be *c*/2, or ~3.44 Å, which will yield a hydrogen bond length (O─H···O) length of 2.49 Å, using the method of Brown and Altermatt (1985) wherein H···O = [(O─O) – 0.95 Å]. That hydrogen bond length yields a hydrogen bond strength of 0.08 v.u. (Ferraris and Ivaldi 1988; all H-bond calculations assume a linear O─H···O sequence, in accord with the $P6_3/m$ symmetry). Thus, a hydroxyl oxygen in end-member hydroxylapatite receives 1.92 v.u. in charge-balancing bonding: [(3 × 0.307) = 0.92 v.u.] (Fig. 2) from Ca2, and a net sum of 1.00 v.u. from the two neighboring H atoms [i.e., (1.00–0.08) v.u. direct donor-H bonding and 0.08 v.u. in H···acceptor hydrogen bonding from the immediately adjacent hydroxyl]. This bond valence sum of 1.92 v.u. is a nearly ideal value for the hydroxyl oxygen. We note that the situation of the incorporation of the first F substituent is essentially an equivalent model

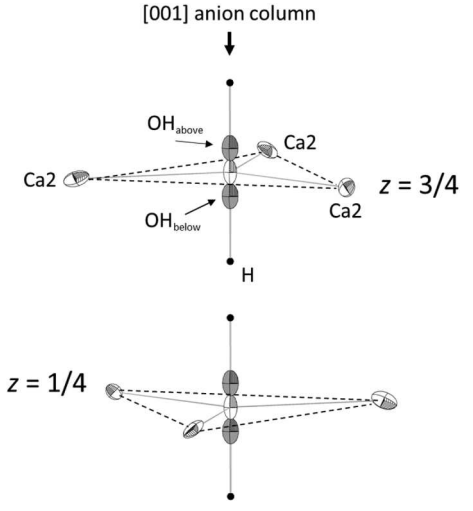

Figure 1. Possible positions of OH and F at anion site in anion column of F-OH apatite. The mirror planes (at $z = ¼, ¾$) in $P6_3/m$ apatite contain the three Ca atoms in the Ca triangle and the F atom in the center of the triangle; Ca-F bonds are shown. The OH (shaded atoms, with bonded black H atoms) positions are ~0.34 Å above or below the mirror plane; the possible Ca2-OH bonds are not depicted. At any intersection of the anion column and a mirror plane, only one of the three depicted anion positions (OH_{above}, F, OH_{below}) is occupied.

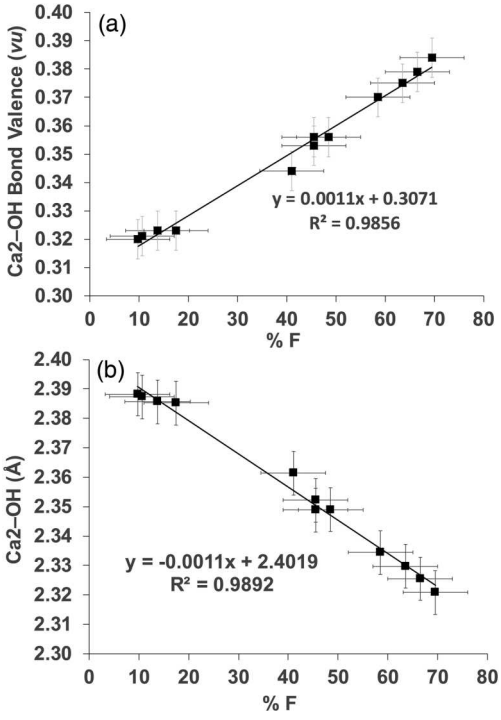

Figure 2. Relationship between Ca2-O(H) bond valence **(a)** and Ca2-O(H) bond distance **(b)** vs. % F in anion column. Samples of 40% F and higher were reported in Hughes et al. (2018).

for fluoridated teeth, as fluoridated human dental enamel incorporates only up to about 2000 ppm of fluorine (Robinson et al. 1996). This model demonstrates the method of stabilization of the fluoride substituent in human teeth.

As fluorine is incorporated into the anion column, the bonding incident upon the column anions changes. Consider the first F atom incorporated into hydroxylapatite. Referring to Figure 1, if that first F ion is incorporated in the mirror plane at $z = ¼$, it will reside in the special position at 0,0,¼. For F, the bonding environment in a hydroxylapatite matrix is "uncomfortable"; the F substituent receives only 0.72 v.u. of charge balance from the surrounding coplanar Ca triangle and thus is significantly underbonded (Fig. 3). This underbonding is alleviated, however, by the hydrogen bonding contributed by neighboring OH ions. Examining the H···F bonding from the H atom associated with the $z = ¾$ hydroxyl, the H···F distance, smaller than the H···O distance between two OH groups because of the displacement of OH, is now ~2.14 v.u. (Fig. 4), yielding a bond valence of 0.10 v.u. (Brown and Altermatt 1985). The F column anion, underbonded with its bonds from Ca, thus gains 0.20 v.u. from H···F hydrogen bonding, contributed from both sides of the F ion, yielding a comfortable bond-valence sum of 0.92 v.u. (Fig. 4).

It is clear that a local fluorine environment must also exist wherein the ion receives H-bonding from only one side in any individual column. Young et al. (1969) suggested that if the sense of the hydroxyl hydrogen was not reversed, and the F received hydrogen bonding from only one direction, the F would be displaced ca. 0.10 Å toward the hydrogen-bonded hydroxyl. Although difficult to observe in diffraction experiments, we did not observe this shift even when the F atom was initially displaced from the special position in the structure modeling. In addition, a 0.10 Å shift of the F ion would yield little additional hydrogen bonding to the F column anion because of the flatness of the hydrogen-bond distance vs. hydrogen-bond

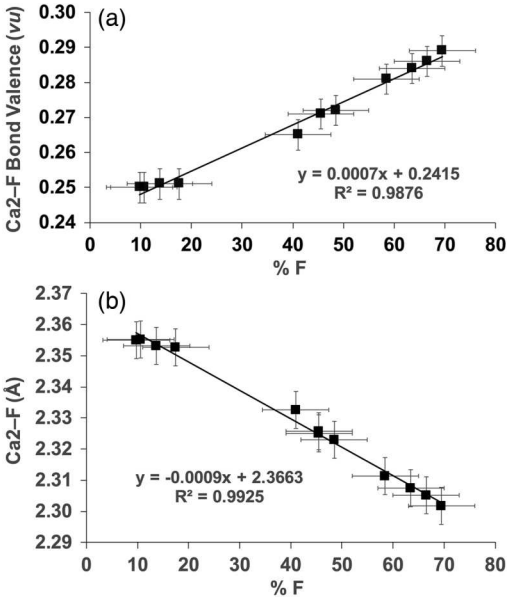

Figure 3. Relationship between Ca2-F bond valence **(a)** and Ca2-F bond distance **(b)** vs. % F in anion column.

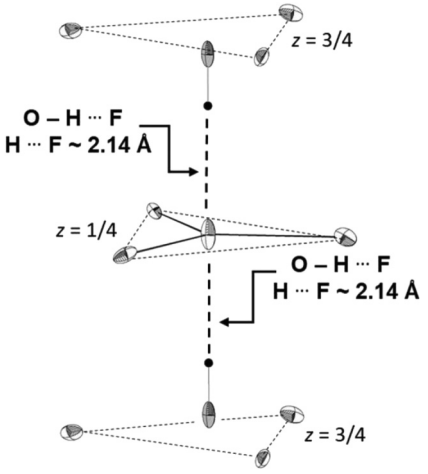

Figure 4. Depiction of O—H···F hydrogen bonding to F column anion occupant adjacent to two OH occupants disordered toward the F occupant.

valence in that region (Brown and Altermatt 1985). Thus, that first F column anion incorporated into hydroxylapatite would have an incident bond valence of 0.82 v.u. if H-bonding was received from one side, as opposed to 0.92 v.u. at a reversal site with incident H-bonding from the ±[001] directions.

Because we know the position of the O(H) atom as a function of F apfu (Fig. 5) and the strength of the bonds to F and O(H) from the surrounding Ca2 atoms (Figs. 2 and 3), we can extend the curves of Hughes et al. (2018) and comment on the incident bond strength to the F and OH column anions over the portion of the F-OH binary that has been synthesized and studied. The bond-valence sum from the surrounding Ca2 atoms to the individual column anions is displayed graphically in Figure 6. As seen therein, at apatite composition of F_0, essentially equivalent to fluoridated dental enamel (which has an F content of approximately $[F_{0.02}(OH)_{99.98}]$), an F column anion is quite underbonded at 0.72 v.u., and a hydroxyl oxygen has a bond valence of 0.92 v.u. The underbonding of the "first F substituent" is modified by 0.20 or 0.10 v.u. of hydrogen bonding, alleviating the underbonding as discussed earlier and allowing the bonding of F substituents to reach acceptable levels. As additional F substitutes, a larger portion of the donor-H direct hydrogen bonding is shed from the average hydroxyl oxygen in the structure to alleviate the underbonding of the additional F ion. Thus, for the average

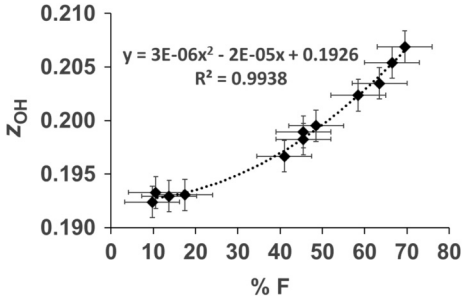

Figure 5. Migration of hydroxyl oxygen as a function of % F in anion column.

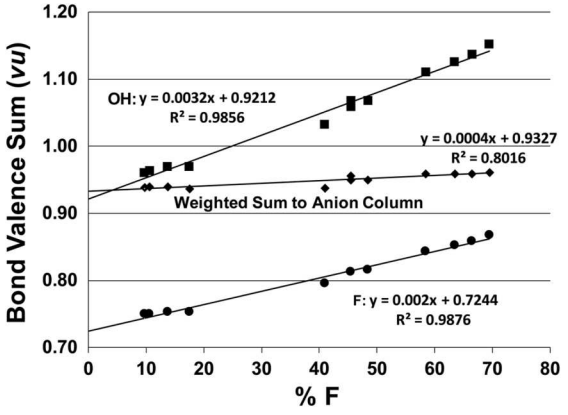

Figure 6. Bond valence from Ca2 triangle contributed to hydroxyl oxygen and F ion in the apatite anion column for varying F compositions. Upper line is the bond valence contributed to column anion sites occupied by OH, lower line is bond valence contributed to column anion sites occupied by F. The middle line, labeled "Weighted Sum to Anion Column," is the actual average bond valence contributed to the anion column for study samples as weighted by anion composition.

hydroxyl, the hydroxyl oxygen must contribute more H-receptor bonding to each substituent F ion, concomitantly reducing the average donor-H bonding to the hydroxyl oxygen. This reduced bonding from the hydrogen to the hydroxyl oxygen must be balanced by increased bonding from the triangle of Ca2 atoms.

As F-content increases in compositions along the join, the decreased donor-H bonding received by the hydroxyl oxygen is compensated by increased bonding from the Ca2 atoms by two methods. Figure 5 illustrates the shift of the O(H) toward its associated mirror plane, thus decreasing the Ca2-OH bond distance and concomitantly increasing the bond valence received by the O(H) column anion from the Ca2 atoms in the (00*l*) triangle of Ca2 atoms. In addition to this shift of the O(H), Figure 7 illustrates the contraction of the Ca2 triangle, also decreasing the Ca2-O(H) distance. The combined effect of these two bond-distance diminutions and concomitant bond-strength increase is illustrated in Figure 2. Figure 6 (middle line) illustrates the remarkable stability in bond valence delivered to the anion column over the range of composition studies. The summed bond valence impingent on column F and OH, weighted by the relative amounts of each anion, sums between 0.93 and 0.96 v.u. over the entire range of samples, not including the intracolumn bonding of 1.00 v.u. for each hydroxyl.

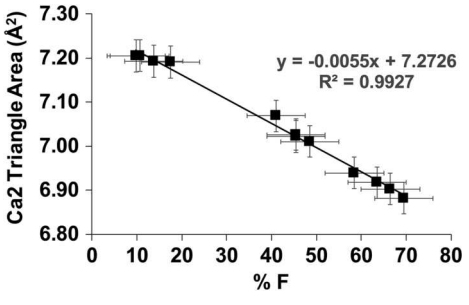

Figure 7. Area of (00*l*) triangles of Ca2 atoms vs. F content.

Implications

The addition of trace amounts of fluoride to human dental enamel has profound effects in preventing dental caries; the process is considered one of the 10 greatest public health accomplishments of the 20th century and places fluoride among the most consumed pharmaceuticals in the world. However, because of the poorly crystallized nature of dental enamel and the difficulty in synthesizing crystals along the F-OH apatite join, considered the best analog of human tooth enamel, the environment of low-concentrations of F in a hydroxylapatite matrix is unknown. This work demonstrates that up to ~25% of the bond valence received by a substituent F column anion is hydrogen bonding; hydrogen bonding is thus essential for the stabilization of F in the apatite column of a hydroxylapatite matrix. The series of crystal structures of apatites along the hydroxylapatite-fluorapatite join presented in Hughes et al. (2018) and this work allow the calculation of bonding environments for column anions along the majority of the F-OH join. The study also illustrates the consistent bond valence delivered to the anion column anionic species over the range of samples studied, as the fluor-hydroxyl atomic arrangement responds to changes in anionic column composition.

Acknowledgments and funding

Support for this work was provided by the National Science Foundation through grants NSF-MRI-1039436 and EAR-1249459 to J.M.H. and EAR-0952298 to J.R. The manuscript was improved by reviews by Giovanni Ferraris and an anonymous reviewer; we greatly appreciate the editorial handling by G. Diego Gatta. J.M.H. would also like to acknowledge the late Maryellen Cameron, a mentor, friend, and colleague with whom he began to examine many aspects of apatite crystal chemistry 40 years ago.

References Cited

Akella, J., Vaidya, S.N., and Kennedy, G.C. (1969) Melting of sodium chloride at pressures to 65 kbar. Physical Review, 185, 1135–1140, https://doi.org/10.1103/PhysRev.185.1135.

American Public Health Association (2021) Community Water Fluoridation (Online). Available: https://www.apha.org/topics-and-issues/fluoridation (accessed October 4, 2021). American Public Health Association.

Aoun, A., Darwiche, F., Al Hayek, S., and Doumit, J. (2018) The fluoride debate: The pros and cons of fluoridation. Preventive Nutrition and Food Science, 23, 171–180, https://doi.org/10.3746/pnf.2018.23.3.171.

Brown, I.D. and Altermatt, D. (1985) Bond-valence parameters obtained from a systematic analysis of the inorganic crystal structure database. Acta Crystallographica. Section B, Structural Science, 41, 244–247, https://doi.org/10.1107/S0108768185002063.

CDC (2021) Community Water Fluoridation (Online). Available: https://www.cdc.gov/fluoridation/php/statistics/?CDC_AAref_Val=https://www.cdc.gov/fluoridation/statistics/index.htm (accessed October 4, 2021). U.S. Centers for Disease Control and Prevention.

Dykes, E. and Elliott, J.C. (1971) The occurrence of chloride ions in the apatite lattice of Holly Springs hydroxyapatite and dental enamel. Calcified Tissue Research, 7, 241–248, https://doi.org/10.1007/BF02062611.

Elliott, J.C., Mackie, P.E., and Young, R.A. (1973) Monoclinic hydroxyapatite. Science, 180, 1055–1057, https://doi.org/10.1126/science.180.4090.1055.

Epple, M., Enax, J., and Meyer, F. (2022) Prevention of caries and dental erosion by fluorides – A critical discussion based on physico-chemical data and principles. Dentistry Journal, 10, 6, https://doi.org/10.3390/dj10010006.

Featherstone, J.D.B. (1999) Prevention and reversal of dental caries: Role of low level fluoride. Community Dentistry and Oral Epidemiology, 27, 31–40, https://doi.org/10.1111/j.1600-0528.1999.tb01989.x.

Ferraris, G. and Ivaldi, G. (1988) Bond valence vs. bond length in O···O hydrogen bonds. Acta Crystallographica. Section B, Structural Science, 44, 341–344, https://doi.org/10.1107/S0108768188001648.

Hughes, J.M., Cameron, M., and Crowley, K.D. (1989) Structural variations in natural F, OH and Cl apatites. American Mineralogist, 74, 870–876.

Hughes, J.M., Cameron, M., and Crowley, K.D. (1990) Crystal structures of natural ternary apatites: Solid solution in the $Ca_5(PO_4)_3X$ (X = F, OH, Cl) system. American Mineralogist, 75, 295–304.

Hughes, J.M., Nekvasil, H., Ustunisik, G., Lindsley, D.H., Coraor, A.E., Vaughn, J., Phillips, B., McCubbin, F.M., and Woerner, W.R. (2014) Solid solution in

the fluorapatite-chlorapatite binary system: High-precision crystal structure refinements of synthetic F-Cl apatite. American Mineralogist, 99, 369–376, https://doi.org/10.2138/am.2014.4644.

Hughes, J.M., Harlov, D., Kelly, S.R., Rakovan, J., and Wilke, M. (2016) Solid solution in the apatite OH-Cl binary system: Compositional dependence of solid solution mechanisms in calcium phosphate apatites along the Cl-OH binary. American Mineralogist, 101, 1783–1791, https://doi.org/10.2138/am-2016-5674.

Hughes, J.M., Harlov, D., and Rakovan, J.F. (2018) Structural variations along the apatite F-OH join. American Mineralogist, 103, 1981–1987, https://doi.org/10.2138/am-2018-6608.

Leventouri, T., Antonakos, A., Kyriacou, A., Venturelli, R., Liarokapis, E., and Perdikatsis, V. (2009) Crystal structure studies of human dental apatite as a function of age. International Journal of Biomaterials, 2009, 698547, https://doi.org/10.1155/2009/698547.

Robinson, C., Kirkham, J., and Weatherell, J.A. (1996) Fluoride in teeth and bone. In O. Fejerskov, J. Ekstrand, and B.A. Burt, Eds., Fluoride in Dentistry, 69–87. Munksgaard.

ten Cate, J.M. and Buzalaf, M.A.R. (2019) Fluoride mode of action: Once there was an observant dentist. Journal of Dental Research, 98, 725–730, https://doi.org/10.1177/0022034519831604.

Young, R.A., van der Lugt, W., and Elliott, J.C. (1969) Mechanism for fluorine inhibition of diffusion in hydroxyapatite. Nature, 223, 729–730, https://doi.org/10.1038/223729a0.

Manuscript received March 15, 2024
Manuscript accepted May 31, 2024
Accepted manuscript online June 12, 2024
Manuscript Handled by G. Diego Gatta

Endnotes:

[1]Deposit item AM-25-39393. Online Materials are free to all readers. Go online, via the table of contents or article view, and find the tab or link for supplemental materials. The CIF has been peer-reviewed by our Technical Editors.